Anal. Bioanal. Electrochem., Vol. 8, No. 5, 2016, 644-657

Analytical & Bioanalytical Electrochemistry

2016 by CEE
www.abechem.com

Full Paper

Effect of Cyclic Potentiodynamic Passivation on the Passive and Electrochemical Behavior of a Mild Carbon Reinforcing Steel in an Alkaline Media Simulating the Concrete Pore Solution

Parviz Mohamadian Samim[1,*] and Arash Fattah-alhosseini[2]

[1] *Department of Materials Engineering, Technical and Vocational University, Hamedan, Iran*

[2] *Department of Materials Engineering, Bu-Ali Sina University, Hamedan 65178-38695, Iran*

*Corresponding Author, Tel.: +98 8132680749; Fax: +98 813280757

E-Mail: parviz.mohamadiansamim@gmail.com

Received: 11 May 2016 / Received in revised form: 26 July 2016 /
Accepted: 1 August 2016 / Published online: 15 August 2016

Abstract- In this work, the effect of cyclic potentiodynamic passivation (CPP) on the passive and electrochemical behavior of a mild carbon reinforcing steel in an alkaline media simulating the concrete pore (0.1 M NaOH+0.1 M KOH) solution was studied by electrochemical impedance spectroscopy (EIS) and Mott–Schottky analysis. Nyquist and Bode plots revealed that the passive film resistance of mild carbon reinforcing steel was increased by applying further CPP cycles. Mott–Schottky analysis showed that the passive films behave as both n-type and p-type semiconductors depending on the potential. Moreover, this analysis revealed that the semiconducting character of the passive films was not altered by CPP method. Also, it was found that both donor densities reduced by increasing the number of CPP cycles. More noble free potentials, smaller cyclic voltammogram loops, larger imperfect semicircles in the Nyquist plots, and less donor densities within the passive film were all indications of the positive effects of CPP. All electrochemical measurements revealed that the electrochemical behavior of mild carbon reinforcing steel was enhanced under the effect of CPP method, mainly attributed to the formation of thicker yet less defective passive films.

Keywords- Mild carbon reinforcing steel, Cyclic potentiodynamic passivation, EIS, Mott–Schottky analysis

1. INTRODUCTION

Generally, the durability of reinforced concrete stems from the excellent chemical stability of hydrated Portland cement and the passivity of mild carbon reinforcing steel in the alkaline concrete pore solutions (pH from 12.5 to 13.5) [1]. Indeed, the enhanced corrosion resistance of mild carbon reinforcing steel in the alkaline concrete pore solution is related to the presence of a very thin passive layer formed on its surface [2–6].

The passive and electrochemical behavior of the passive film formed on the steel and stainless steel is of great importance, which controls the passivity and, therefore the corrosion behavior [5–12]. In practice, the passive and electrochemical behavior depends on several variables including the temperature, immersion time, pH, and the exact composition of the solution in which the passive films are formed [13]. In the last decade, several interesting studies have been published, which focuses on the passive and electrochemical behavior of the passive film formed on the carbon steel in media simulating concrete pore solutions [5, 6].

A wide number of methods including chemical, mechanical, and electrochemical processes have been used to improve the surface characteristics (especially corrosion resistance) of metals and alloys [14,15]. One of the electrochemical surface modification methods, which have been less studied, is the CPP. This technique can be fast, cost effective, and environmentally friendly for corrosion protection. Shahryari et al. [16–18] have shown that general and pitting corrosion resistance of AISI 316LVM stainless steel was enhanced through the application of CPP method. Also, it was revealed that the surfaces of AISI 316LVM stainless steel, which were modified by CPP method, offered a better corrosion resistance when compared with the unmodified surfaces. In other study, Vuković has reported that CPP method increased the passive layer stability of AISI 302 stainless steel in an alkaline media [19].

Since the effect of CPP method on the electrochemical behavior of carbon steels has been less studied, this work was attempted to evaluate the efficacy of CPP method on the electrochemical behavior of mild carbon reinforcing steel in the alkaline media simulating the concrete pore (0.1 M NaOH+0.1 M KOH) solution.

2. EXPERIMENTAL PROCEDURES

Table 1 shows the chemical compositions of the steel. To prepare the working electrode, a 2 cm×2 cm sample was cut from a 0.3 cm thick sheet and then one of its rolling surfaces was well ground with the abrasive papers (from 100 to 2000 grit) to reveal a smooth surface. After grinding the surface sample, it was washed with distilled water, and finally dried with cold air stream. It is worth nothing that the construction of the flat cell used for the electrochemical tests was such that only a limited area of the sample surface (i.e 0.64 cm^2)

was subjected to the solution. The schematic representation of the above description is shown in Fig. 1.

Table 1. Chemical composition of mild carbon reinforcing steel

	C	**Mn**	**P**	**Ti**	**Fe**
Mild carbon Steel/ wt%	0.28	1.20	0.30	0.04	Bal

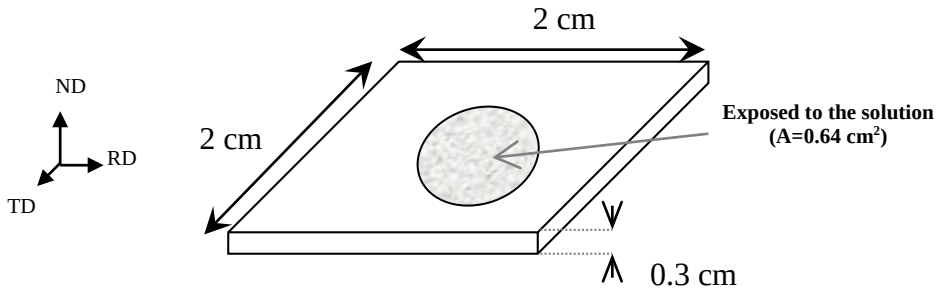

Fig. 1. The schematic illustration of the working electrode together with the location of the exposed area of the surface

For each electrochemical experiment, the mild carbon reinforcing steel samples, an Ag/AgCl electrode (in saturated KCl solution), and a platinum wire were set as working, reference, and counter electrodes, respectively, in a conventional three-electrode flat cell configuration. A μAutolab Type III/FRA2 system controlled by a personal computer was used for all of the electrochemical measurements. All experiments were carried out at room temperature in a 0.1 M NaOH+0.1 M KOH solution using analytical grade chemicals and distilled water. The detailed procedures of the electrochemical tests and their conditions are as follows:

(1) The open-circuit potential (OCP) was measured to register the variation of surface potential within 1800 s, and to ensure that steady state condition was reached for the execution of subsequent tests. (2) Potentiodynamic polarization plots were measured between the potential range of -0.25 V (vs. E_{corr}) and 0.7 $V_{Ag/AgCl}$. (3) CPP was applied at a scan rate of 50 mVs^{-1} and in the passive domain of this alloy (i.e. 0.0 to 0.6 $V_{Ag/AgCl}$). (4) The OCP was measured again for 900 s to ascertain that steady state condition was reached after applying CPP. (5) Mott–Schottky tests were performed at a frequency of 1 kHz and with a 10 mV AC signal. The potential was swept in the cathodic direction with a step potential of 25 mV and in the potential range of 0.6 to -0.9 $V_{Ag/AgCl}$. (6) EIS tests were recorded between the frequency range of 100 kHz and 10 mHz and with a sinusoidal amplitude of 10 mV. To model the EIS data and curve-fitting, the NOVA impedance software was used.

3. RESULTS AND DISCUSSION

3.1. Potentiodynamic Polarization Measurements

Fig. 2a depicts the changes in OCP values as a function of immersion time in the alkaline media simulating the concrete pore (0.1 M NaOH+0.1 M KOH) solution for mild carbon reinforcing steel samples. It is observed that the free potential gently shifted toward nobler values. Such an OCP profile shows that the passive film was forming gradually [20]. After this initial step, potentiodynamic polarization could be measured. The potentiodynamic polarization plot of mild carbon reinforcing steel samples in the alkaline media simulating the concrete pore solution is shown in Fig. 2b. As can be seen, an appropriate potential range was chosen to perform CPP.

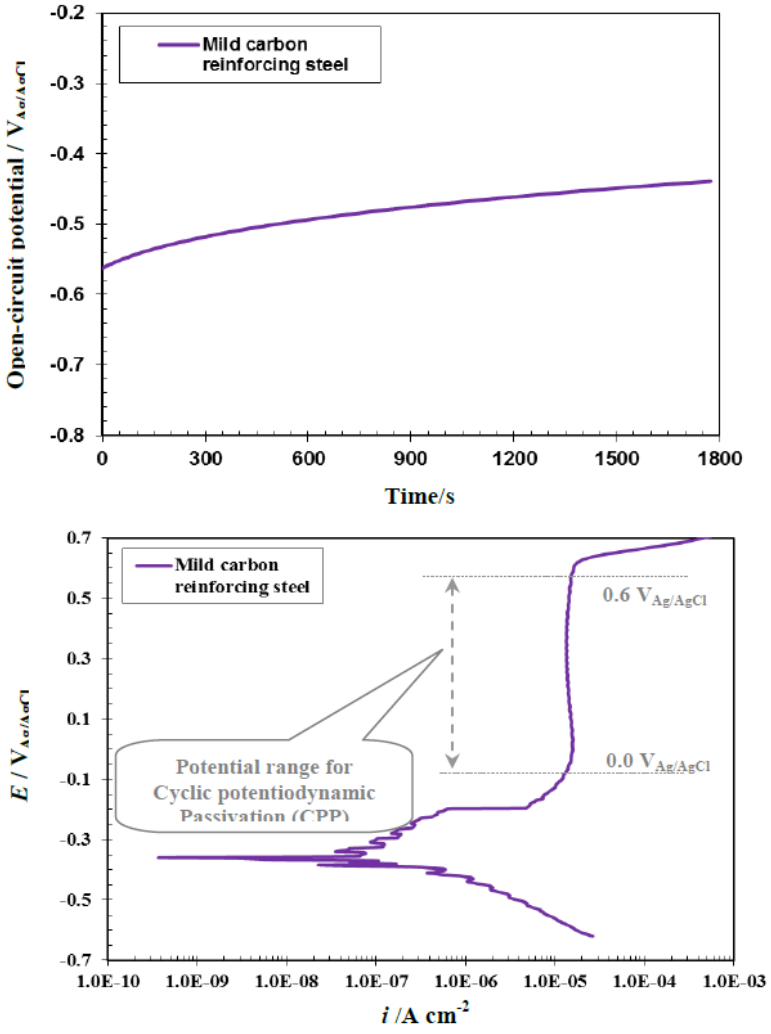

Fig. 2. (a) The OCP and (b) potentiodynamic polarization curves of mild carbon reinforcing steel sample in the alkaline media simulating the concrete pore (0.1 M NaOH+0.1 M KOH) solution (scan rate = 1 mVs^{-1})

3.2. Cyclic Potentiodynamic Passivation

Fig. 3 shows the evolution of cyclic voltammetry loops of mild carbon reinforcing steel samples in the alkaline media simulating the concrete pore solution for a different number of cycles in the potential region between –0.2 $V_{Ag/AgCl}$ and 0.9 $V_{Ag/AgCl}$. As it is seen, as the number of polarization sweep cycles increased, smaller or nobler loops were formed. Indeed, the dependence of current density on passive potential decreased at a higher number of cycles, representing stable passive layers were formed on the surface of the sample.

It is worth mentioning that the chemical composition of the passive layer is based on iron oxides such as ferrous hydroxide ($Fe(OH)_2$), magnetite (Fe_3O_4) and hematite (Fe_2O_3). The stability of these oxides is such that at more anodic potentials than the formation of magnetite, Fe_2O_3 is formed, while at more cathodic potentials than the formation of magnetite, $Fe(OH)_2$ is formed [21 and 22].

$$Fe + 2OH^- \leftrightarrow Fe(OH)_2 \quad (1)$$

$$3Fe(OH)_2 + 2OH^- \leftrightarrow Fe_3O_4 + 4H_2O + 2e^- \quad (2)$$

$$2Fe_3O_4 + 2OH^- \leftrightarrow 3Fe_2O_3 + H_2O + 2e^- \quad (3)$$

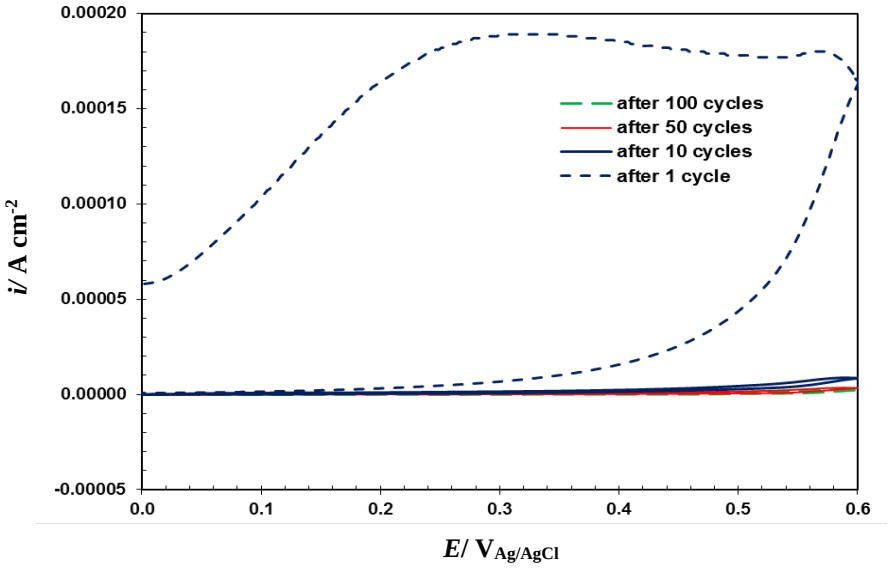

Fig. 3. The comparison of CPP plots of mild carbon reinforcing steel samples in the alkaline media simulating the concrete pore solution for a different number of cycles

3.3. OCP Measurements

Upon the completion of CPP, subsequent electrochemical tests cannot be run unless a new steady-state situation is attained. Hence, OCP measurements are necessary for the determination of sufficient time to reach a stable condition. The rationale behind this approach is two-fold. First, understanding how CPP changes surface potential of the samples

and when the potential stabilization is reached. Second, to ensure a steady-state condition is attained for the execution of subsequent tests, i.e. EIS and Mott–Schottky analysis. The OCP curves acquired after each distinct cycle of CPP for mild carbon reinforcing steel samples in the alkaline media simulating the concrete pore (0.1 M NaOH+0.1 M KOH) solution are shown in Fig. 4. The corresponding OCP plots of mild carbon reinforcing steel samples reveal a distinct positive shift compared to the unmodified sample (Fig. 1a). As it is seen, as the number of CPP cycles increased, the OCP level is increased. This positive shift in the free potential shows the beneficial effect of CPP method on the formation of a more protective passive film.

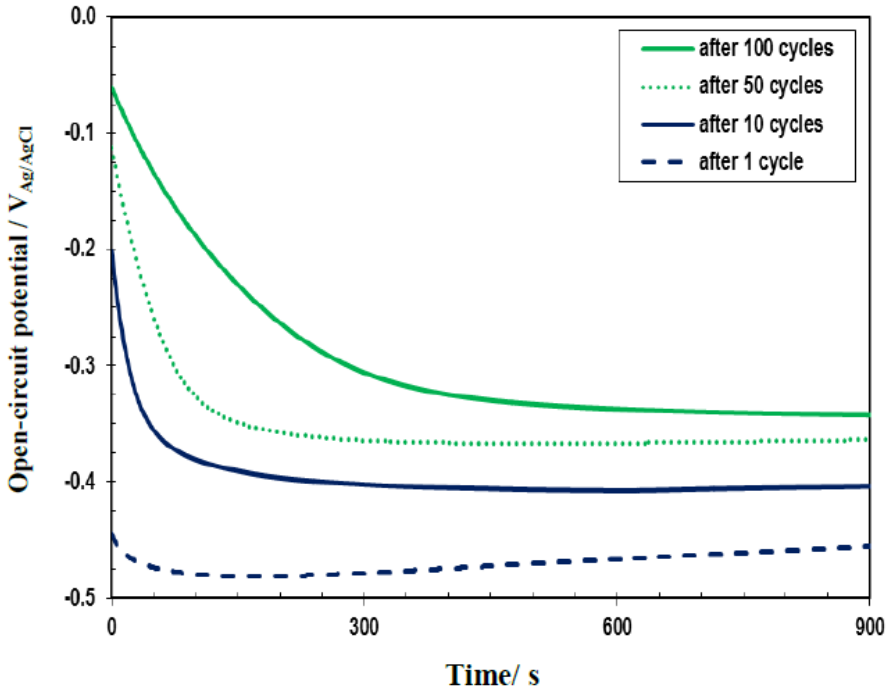

Fig. 4. The OCP curves after different cycles for mild carbon reinforcing steel samples

3.4. EIS Measurements

After applying a different number of polarization sweep cycles (1, 10, 50, and 100) and allowing the surface potential to attain the steady-state condition, mild carbon reinforcing steel samples were studied by EIS tests (Fig. 5). The beneficial effect of the higher number of CPP cycles can be observed in the semicircles of Nyquist plots (Fig. 5a), where they became larger and more imperfect. Based on the bode-magnitude plots (Fig. 5b), a marked capacitive behavior can be seen in the low to the middle-frequency range. This behavior heightened as the number of cycles increased. Also, larger phase angles remained in a wider frequency range under the effect of the higher number of CPP cycles.

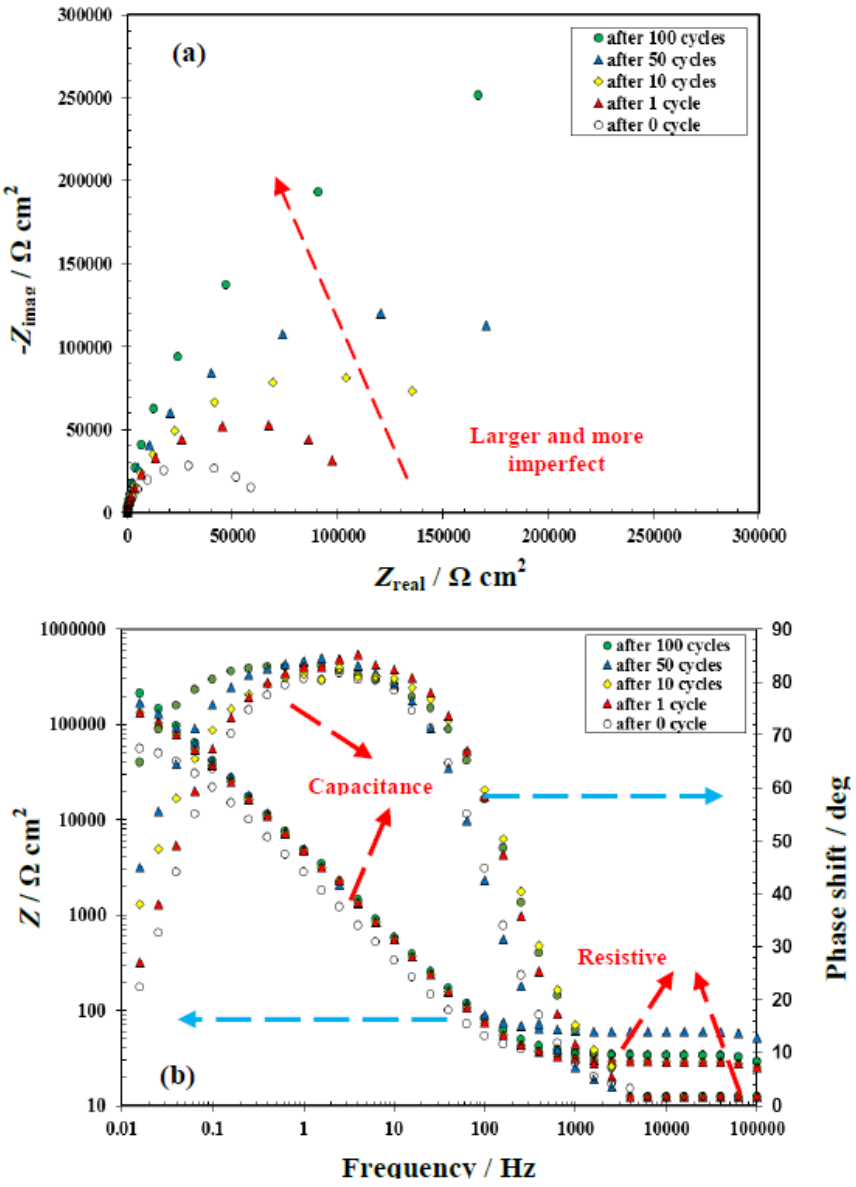

Fig. 5. (a) Nyquist and (b) Bode plots of mild carbon reinforcing steel samples obtained after a different number of cycles

For the validation of EIS results, the Kramers–Kronig transformation was used. The importance and exact details of applying Kramers–Kronig transformation have been discussed elsewhere [23]. Fig. 6 shows the typical Kramers–Kronig transformations corresponds to mild carbon reinforcing steel samples after 0, 1, 10, 50, and 100 cycles of CPP. Clearly, Fig. 6 validates the conformity of the system studied herein with the prerequisites of linear system theory [24].

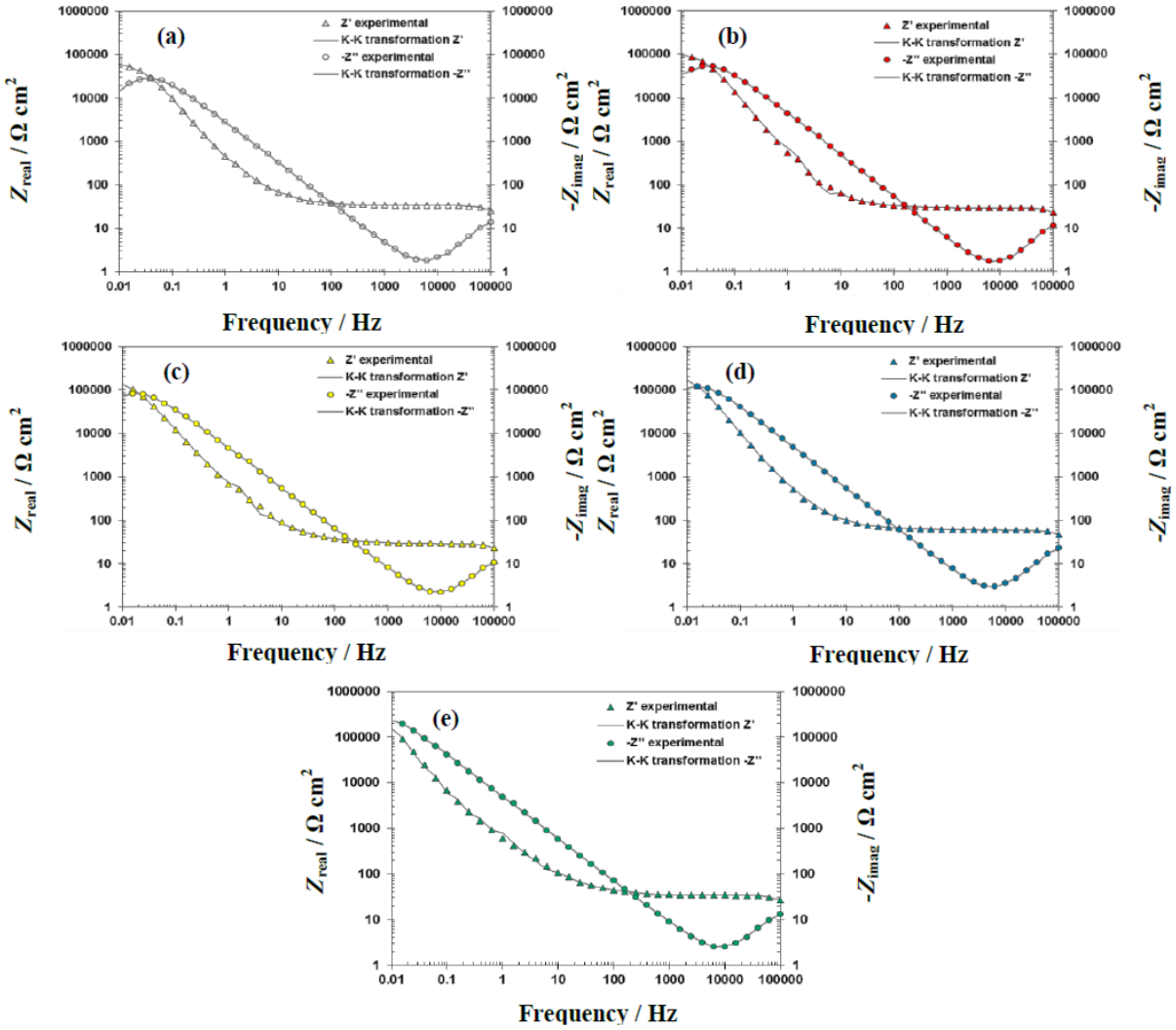

Fig. 6. Kramers–Kronig plots of mild carbon reinforcing steel samples obtained after different numbers of cycles, (a) 0 cycle, (b) 1 cycle, (c) 10 cycles, (d) 50 cycles, and (e) 100 cycles

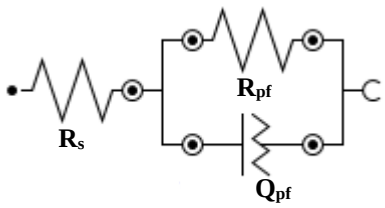

Fig. 7. The best equivalent circuit used for modeling of the EIS spectrum

Considering different representations of impedance data (Fig. 5), just one-time constant was sufficient to describe the EIS plots. Therefore, the EIS plots were modeled by the

equivalent electrical circuit (EEC) shown in Fig. 7. This EEC has been used to model the electrochemical behavior of stainless steels in other alkaline solutions [25,26].

The definitions of circuit elements are as follows: R_s shows the solution resistance, R_{pf} represents the resistance of the passive film, and Q_{pf} denotes the constant phase element (CPE) corresponding to the capacitance of the passive film.

The evolution of R_{pf} for mild carbon reinforcing steel samples in the alkaline media simulating the concrete pore solution is illustrated in Fig. 8a. Obviously, as the number of CPP cycles increased, the polarization resistance of passive films increased. This ascending trend clearly reveals that the protectiveness of passive films was enhanced under the influence of CPP method. Here, it should be mentioned that the impedance and admittance of CPE are obtained by the following equations [27]:

$$Z_{CPE} = [Y_0(j\omega)^n]^{-1} \quad (4)$$

$$Y_{CPE} = Y_0(j\omega)^n \quad (5)$$

Where j shows the imaginary unit, ω represents the angular frequency, and n is defined as the CPE exponent, which is adjusted between 0 and 1. At extreme values of 1 or 0, the CPE shows an ideal capacitor or an ideal resistor, respectively. For n=0.5, the CPE represents a Warburg impedance with a diffusion character. CPE indicates a capacitive element when n varies between 0.5 and 1. Generally, the CPE describes a frequency dispersion of time constants attributed to local surface inhomogeneities, roughness, and the like. The capacitance of the passive film (C_p) can be estimated by considering Hsu-Mansfeld's formula which as follows [28]:

$$C_p = Y_0(j\omega_m^{''})^{n-1} \quad (6)$$

Where $\omega_m^{''}$ shows the angular frequency at the imaginary part of the impedance has its maximum value. Ergo, the thickness of the passive film (d) can be determined from extracted values of C_p. The thickness of passive film can be obtained by the following equation [29]:

$$d = \frac{\varepsilon\varepsilon_0 A}{C} \quad (7)$$

Where C represents the capacitance of passive film, ε shows the dielectric constant, ε_0 is the vacuum permittivity, and A shows the effective surface area. Concerning this equation, Luo et al. has pointed out that dielectric constant of the passive film may vary with it composition, consequently, an accurate measurement of the passive film thickness by EIS data is difficult [29]. Considering the above equation, nevertheless, the evolution of film thickness could be estimated rather than reporting absolute values of film thickness. In line with that, the evolution of C_p is shown in Fig. 8b. A descending trend is observable for the

capacitance; hence, one expects an ascending trend for the passive film thickness with respect to the number of CPP cycles. In brief, EIS results showed that the electrochemical behavior of mild carbon reinforcing steel in the alkaline media simulating the concrete pore (0.1 M NaOH + 0.1 M KOH) solution was improved under the influence of CPP method, mainly due to the formation of thicker protective passive films.

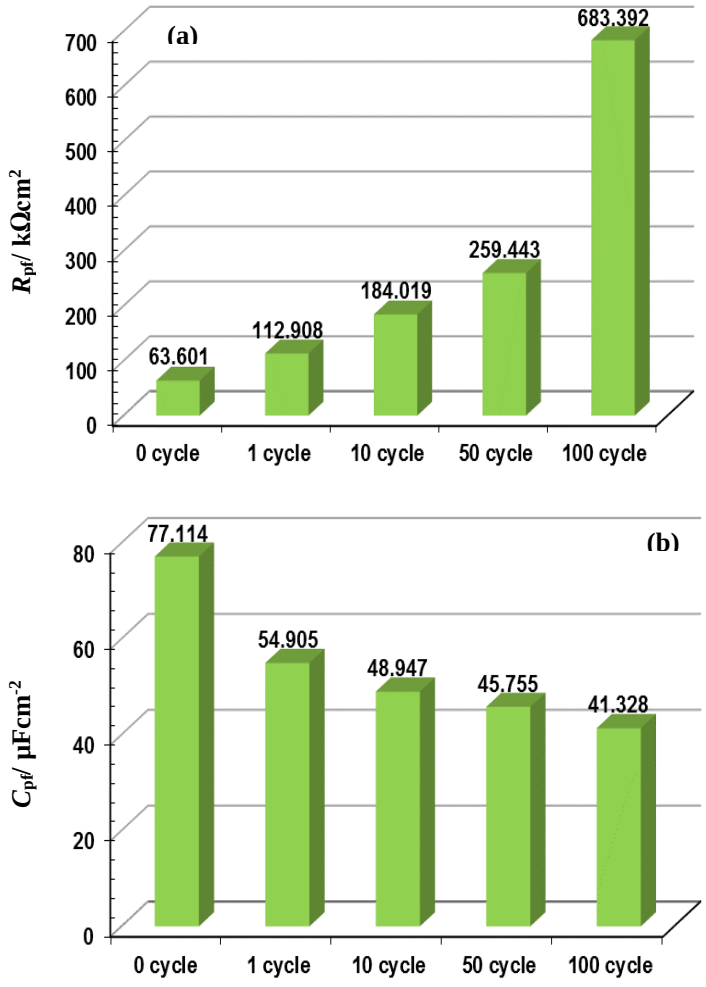

Fig. 8. Variations in the (a) passive film resistance and (b) double layer capacitance of mild carbon reinforcing steel samples

3.5. Mott–Schottky Analysis

Generally, passive films are non-stoichiometric compounds having semiconductive characteristics. The semiconductivity of these films stems from the existence of point defects, which are charge carriers. While n-type semiconductivity is caused by metal interstitials and oxygen vacancies acting as electron donors, cation vacancies as electron acceptors result in p-type semiconductivity [30–34].

The Mott–Schottky analysis is one of the most powerful methods to investigate the semiconductive properties of passive films. The Mott–Schottky relationships (Eq. 5 and 6) show the relation between the inverse square of the space charge capacitance and the applied voltage. These equations are used to specify the semiconductor type and determine charge carrier densities of the passive films [30–38]:

$$\frac{1}{C^2} = \frac{2}{\varepsilon\varepsilon_0 e N_D}\left(E - E_{FB} - \frac{kT}{e}\right) \qquad \text{for n-type semiconductor} \qquad (8)$$

$$\frac{1}{C^2} = -\frac{2}{\varepsilon\varepsilon_0 e N_A}\left(E - E_{FB} - \frac{kT}{e}\right) \qquad \text{for p-type semiconductor} \qquad (9)$$

where N_D and N_A show the concentration of the electron donors and acceptors, ε_0 accounts for the permittivity of the free space, ε stands for the dielectric constant of the passive film, T shows the absolute temperature, k denotes the Boltzmann constant, e is the electron charge, and E_{FB} is the flat band potential.

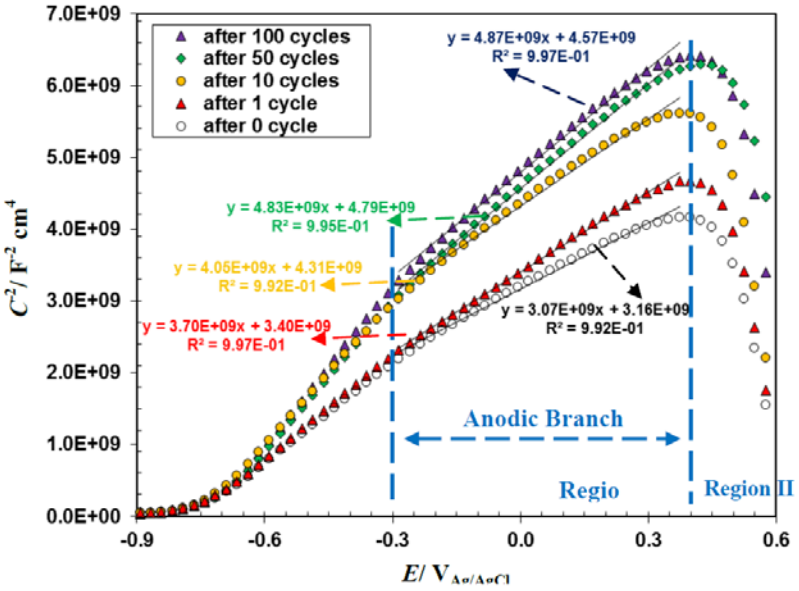

Fig. 9. Mott–Schottky plots of mild carbon reinforcing steel samples obtained after different numbers of cycles

The Mott–Schottky plots of mild carbon reinforcing steel samples obtained after applying a different number of potentiodynamic polarization sweep cycles in the alkaline media simulating the concrete pore solution are shown in Fig. 9. In all curves, two main regions with different slopes can be distinguished. The positive slopes of the potential region (I) are due to n-type behavior, while negative slopes of the potential region (II) are due to p-type behavior. All samples have general semiconducting properties because of the resemblance existing in the shapes of their Mott–Schottky curves, but the main dissimilarity is due to

different slopes of Mott–Schottky curves causing the difference in donor and acceptor concentration.

Considering the equation 8 and Fig. 9, the slopes of linear regions (I) can be obtained, thereby, donor densities can be estimated. The estimation of donor concentrations for mild carbon reinforcing steel samples after applying a different number of polarization sweep cycles is presented in Fig. 10. The donor densities are in the order of magnitude ~10^{21} cm^{-3}. As it is seen, as the number of applied cycles increased, the donor densities decreased. Interestingly, applying CPP led to a reduction in the number of point defects within the passive film. In fact, this implies that the passive films formed under the influence of CPP were less defective.

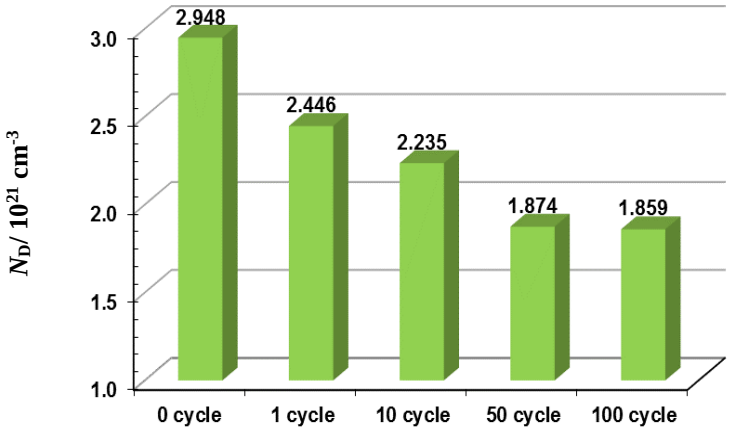

Fig. 10. Variations in the donor densities of mild carbon reinforcing steel samples in the alkaline media simulating the concrete pore solution

4. CONCLUSION

This work aimed to study the efficacy of cyclic potentiodynamic passivation (CPP) method as a surface modification method on the passive and electrochemical behavior of mild carbon reinforcing steel in the alkaline media simulating the concrete pore (0.1 M NaOH+0.1 M KOH) solution. CPP method was very satisfactory to improve the passivity of mild carbon reinforcing steel samples. Applying polarization sweeps up to 100 cycles gave rise to several noteworthy changes including shrinkage of voltammogram loops, approaching nobler OCP values, an ascending trend in resistive terms, a descending trend in capacitive terms, a descending trend in the concentration of point defects. These are all explicit indications of a drastic enhancement of passive behavior and resistance to corrosion. On the whole, CPP has led to the formation of thicker yet less defective passive films.

REFERENCES

[1] B. Elsener, D. Addari, S. Coray, and A. Rossi, Electrochim. Acta 56 (2011) 4489.
[2] J. Williamson, and O. B. Isgor, Corros. Sci. 106 (2016) 82.
[3] M. Criado, I. Sobrados, J. Sanz, and J. M. Bastidas, Sur. Coat. Technol. 258 (2014) 485.
[4] H. Sun, L. Wei, M. Zhu, N. Han, J. H. Zhu, and F. Xing, Const. Build. Mater. 112 (2016) 538.
[5] J. Shi, W. Sun, J. Jiang, and Y. Zhang, Const. Build. Mater. 111 (2016) 805.
[6] A. Poursaee, and C. M. Hansson, Cem. Concr. Res. 37 (2007) 1127.
[7] N. E. Hakiki, M. Da Cunha Belo, A. M. P. Simões, and M. G. S. Ferreira, J. Electrochem. Soc. 145 (1998) 3821.
[8] M. Da Cunha Belo, N. E. Hakiki, and M. G. S. Ferreira, Electrochim. Acta 44 (1999) 2473.
[9] K. Sugimoto, and Y. Sawada, Corros. Sci. 17 (1997) 425.
[10] M. F. Montemor, A. M. P. Simões, M. G. S. Ferreira, and M. Da Cunha Belo, Corros. Sci. 41 (1999) 17.
[11] N. E. Hakiki, S. Boudin, B. Rondot, and M. Da Cunha Belo, Corros. Sci. 37 (1995) 1809.
[12] C. M. Rangel, T. M. Silva, and M. Da Cunha Belo, Electrochim. Acta 50 (2005) 5076.
[13] C. O. A. Olsson, and D. Landolt, Electrochim. Acta 48 (2003) 1093.
[14] H. S. Khatak, B. Raj, Corrosion of austenitic stainless steels: mechanism, mitigation and monitoring, Elsevier, (2002).
[15] X. Liu, P. K. Chu, and C. Ding, Mater. Sci. Eng. R 47 (2004) 49.
[16] A. Shahryari, F. Azari, H. Vali, and S. Omanovic, Phys. Chem. Chem. Phys. 11 (2009) 6218.
[17] A. Shahryari, S. Omanovic, and J. A. Szpunar, J. Biomed. Mater. Res. Part A 89 (2009) 1049.
[18] A. Shahryari, W. Kamal, and S. Omanovic, Mater. Lett. 62 (2008) 3906.
[19] M. Vuković, Corros. Sci. 37 (1995) 111.
[20] E. E. Oguzie, J. Li, Y. Liu, D. Chen, Y. Li, K. Yang, and F. Wang, Electrochim. Acta 55 (2010) 5028.
[21] M. Sánchez, J. Gregori, C. Alonso, J. J. García-Jareño, H. Takenouti, and F. Vicente, Electrochim. Acta 52 (2007) 7634.
[22] A. Esen, T. Kosec, A. Legat, and V. Bokan-Bosiljkov, Mater. Technol.48 (2014) 51.
[23] A. Fattah-alhosseini, and S. Vafaeian, J. Alloys Comp. 639 (2015) 301.
[24] C. Escrivà-Cerdán, E. Blasco-Tamarit, D.M. García-García, J. García-Antón, and A. Guenbour, Electrochim. Acta 80 (2012) 248.
[25] Z. Feng, X. Cheng, C. Dong, L. Xu, and X. Li, J. Nucl. Mater. 407 (2010) 171.
[26] Z. Feng, X. Cheng, C. Dong, L. Xu, and X. Li, Corros. Sci. 52(11) (2010) 3646.

[27] D. G. Li, J. D. Wang, D. R. Chen, and P. Liang, Ultrason. Sonochem. 29 (2016) 48.
[28] C. H. Hsu, and F. Mansfeld, Corrosion 57 (2001) 747.
[29] H. Luo, S. Gao, C. Dong, and X. Li, Electrochim. Acta 135 (2014) 412.
[30] R.M. Fernández-Domene, E. Blasco-Tamarit, D. M. García-García, and J. García-Antón, Thin Solid Films 558 (2014) 252.
[31] A. Fattah-alhosseini, M. A. Golozar, A. Saatchi, and K. Raeissi, Corros. Sci. 52 (2010) 205.
[32] A. Fattah-alhosseini, A. Saatchi, M. A. Golozar, and K. Raeissi, J. Appl. Electrochem. 40 (2010) 457.
[33] Y. Zhang, M. Urquidi-Macdonald, G. R. Engelhardt, and D. D. Macdonald, Electrochim. Acta 69 (2012) 1.
[34] S. Yang, and D. D. Macdonald, Electrochim. Acta 52 (2007) 1871.
[35] H. Luo, C. F. Dong, K. Xiao, and X. G. Li, Appl. Surf. Sci. 258 (2011) 631.
[36] L. Jinlong, and L. Hongyun, Appl. Surf. Sci. 280 (2013) 124.
[37] L.V. Jin-long, and L. Hong-yun, Mater. Chem. Phys. 135 (2012) 973.
[38] L. Jinlong, and L. Hongyun, Appl. Surf. Sci. 263 (2012) 29.